frontiers | Frontiers in Materials

TYPE Mini Review
PUBLISHED 28 September 2022
DOI 10.3389/fmats.2022.1010156

OPEN ACCESS

EDITED BY
Vadim G. Kessler,
Swedish University of Agricultural Sciences, Sweden

REVIEWED BY
Bo Wang,
Hebei University of Science and Technology, China

*CORRESPONDENCE
Daniela V. Lopes,
daniela.rosendo.lopes@ua.pt
Andrei V. Kovalevsky,
akavaleuski@ua.pt

SPECIALTY SECTION
This article was submitted to Ceramics and Glass, a section of the journal Frontiers in Materials

RECEIVED 02 August 2022
ACCEPTED 13 September 2022
PUBLISHED 28 September 2022

CITATION
Lopes DV, Quina MJ, Frade JR and Kovalevsky AV (2022), Prospects and challenges of the electrochemical reduction of iron oxides in alkaline media for steel production. *Front. Mater.* 9:1010156. doi: 10.3389/fmats.2022.1010156

Prospects and challenges of the electrochemical reduction of iron oxides in alkaline media for steel production

Daniela V. Lopes[1]*, Margarida J. Quina[2], Jorge R. Frade[1] and Andrei V. Kovalevsky[1]*

[1]Department of Materials and Ceramic Engineering, CICECO—Aveiro Institute of Materials, University of Aveiro, Aveiro, Portugal, [2]CIEPQPF, Department of Chemical Engineering, Pólo II—Pinhal de Marrocos, University of Coimbra, Coimbra, Portugal

Steelmaking industries have been facing strict decarbonization guidelines. With a net zero carbon emissions target, European policies are expected to be accomplished before 2050. Traditional steelmaking industry still operates by the carbothermic reduction of iron ores for steel production. Consequently, the steel sector is responsible for a large amount of CO_2 emissions, accounting for up to 9% of the CO_2 worldwide emissions. In this scope, the electrochemical reduction or electrolysis of iron oxides into metallic iron in alkaline media arises as a promising alternative technology for ironmaking. Significant advantages of this technology include the absence of CO_2 emissions, non-polluting by-products such as hydrogen and oxygen gases, lower temperature against the conventional approach (~100°C *versus* 2000°C) and lower electric energy consumption, where around 6 GJ per ton of iron manufactured can be spared. The present minireview discusses the progress on the electrochemical reduction of iron oxides in alkaline media as a green steelmaking route. A historical overview of the global steelmaking against recent developments and challenges of the novel technology is presented, and the fundamental mechanisms of iron oxide reduction to iron and alternative iron feedstocks are discussed. Factors affecting the Faradaic efficiencies of the alkaline electroreduction of iron oxide suspensions or iron oxide bulk ceramics are also explored, focusing on the concurrent hydrogen evolution reaction. Overall, if scrutinized, this technology may become a breaking point for the steel industry sector.

KEYWORDS

electrowinning, steelmaking, iron ore, green steel, carbon free technology

Introduction

The Sustainable Development Goals proposed by the United Nations General Assembly and the European Green Deal provide an integrated roadmap for making the World and EU's economy more sustainable, emphasizing the role of transition to clean and renewable energy sources and carbon-neutral technologies. Large industries, like steel, face strong pressure to lower greenhouse gas emissions (Elavarasan et al., 2022). Thus, high investments in developing alternative technologies, preferably relying on renewable energy, are required. About 1951 million tonnes of crude steel were produced worldwide in 2021, with expected growth in the upcoming years (World Steel Association, 2022). The Blast Furnace coupled with a Basic Oxygen Furnace (BF-BOF) is responsible for 71% of the total steel production during the conventional carbothermic reduction of iron ores with coke to "pig iron" at high temperatures (1,500°C and 1,650 °C when considering BOF). The remaining 29% are related to non-coke-based technologies such as the Electric Arc Furnace (EAF) and the Direct Reduced Iron (DRI). Despite the associated CO_2 emissions, the BF-BOF is expected to continue to be the primary route for steelmaking in the upcoming years due to the high mass production capacity and cost-effectiveness (HORIZON 2020, 2020; Fan and Friedmann, 2021). The resulting emissions account for about 7–9% of the global CO_2 emissions. Due to the demanding steel production rate, 3.0 billion tonnes of CO_2 emissions are estimated for 2050 (Mousa, 2019). Thus, the steelmaking industry is under great strain to improve its technology regarding the use of less raw materials, less energy consumption, lower emissions of particles and gas, and opening new routes for CO_2-lean steelmaking.

Electrolysis of metal oxides for metal production arises as a greener approach to conventional extraction methods, offering advantages such as the absence of CO_2 emissions, non-polluting by-products such as hydrogen and oxygen gases, and lower electric energy consumption (13 GJ/ton of Fe against 19 GJ/ton (Beer et al., 2000; Allanore et al., 2010b). Electrolysis is a conventional technology nowadays for producing aluminium (Mandin et al., 2019), zinc (Monhemius, 1980), and other metals. Several potentially positive impacts of electrolytic iron production were identified in SIDERWIN project (SIDERWIN, 2022), including 87% reduction in direct CO_2 emissions, 31% reduction in energy use, the ability to involve iron oxide-containing residues like red mud, and potential compatibility with renewable energies.

A brief historical perspective

Attempts toward electrolytic iron production undertaken in the last century have identified several challenges. It was firstly reported in patents considering alkaline solutions (Estelle, 1915; Angel, 1952), followed by electroplating in acidic baths (Shafer and Harr, 1958; Izaki, 2010; Gamburg and Zangari, 2011) for iron strips and electrotypes manufacturing in the early 30s. Electrolyte ferrous solutions ($FeSO_4$ or $FeCl_2$ at pH ranges of 0.5–5.5) were electrolyzed at temperatures below 100°C. However, light grey and brittle deposits were frequently obtained, even with the addition of Al-Mg-Na sulphates, $Fe(BF_4)_2$ or $Fe(H_2NO_3S)_2$. The pitted iron deposits were observed under acidic conditions, since Fe^{2+} and Fe^{3+} co-exist in the acidic electrolytic bath, forming a redox cycle loop between the iron species, lowering the overall Faradaic efficiency (Pourbaix, 1974; Allanore et al., 2010c; Izaki, 2010). Few studies have been performed in recent years, except for a few efforts with fluorborate (Su et al., 2009) and sulphate (Díaz et al., 2008) acidic media. The electrolytic iron production was then mainly investigated considering the alkaline conditions. However, little attention has been paid to this process mostly due to the doubtful mechanism of reduction to Fe (Gorbunova and Liamina, 1966). Until now, questions about the relatively low electrolysis temperature (≈100 °C), insulating properties of Fe_2O_3 (Morin, 1951; Lee et al., 2012), 10^{-14} S/cm, the low solubility of the iron oxides, and presumably single reduction step ($Fe_2O_3 + 3H_2O + 6e^- \rightarrow 2Fe^0 + 6OH^-$), have been the reasons to doubt the prospects of this electrolytic process (Cornell and Schwertmann, 2003; Allanore et al., 2007, 2008).

Significant advances have been made in the last two decades. Iron oxide electrolysis in alkaline aqueous solutions is now considered one of the most promising technologies for iron production (Monteiro et al., 2016; Müller et al., 2016; Ivanova et al., 2017; Cavaliere, 2019). Several large R&D projects have been approved during the last decade seeking alternative CO_2-free technologies with low energy consumption, such as IERO, ULCOS, LowCarbonFuture, GREENSTEEL, among many others (U.S. Department of Energy, 2014; Lavelaine et al., 2016; Quader et al., 2016; Draxler et al., 2020). The ongoing project on low-temperature electrolysis for steel production, SIDERWIN (SIDERWIN, 2022), has been strongly encouraged by the European Commission under the Horizon 2020, where the first pilot-scale plant for iron production by electrolysis of iron oxide-containing suspensions is being developed.

Fundamental mechanisms and current research trends

Experimentally, there are two approaches for electroreduction (Figure 1): the electrodeposition of Fe on a working electrode (WE, e.g., Ni (Figure 1A) from iron oxide-based suspensions; or the electroreduction of a bulk iron oxide-based cathode (porous or dense, Figure 1B). Cathodes morphologies before and after reduction are also represented in Figure 1, attending to each type of electroreduction. The iron formation mechanisms and corresponding microstructural evolution are discussed below.

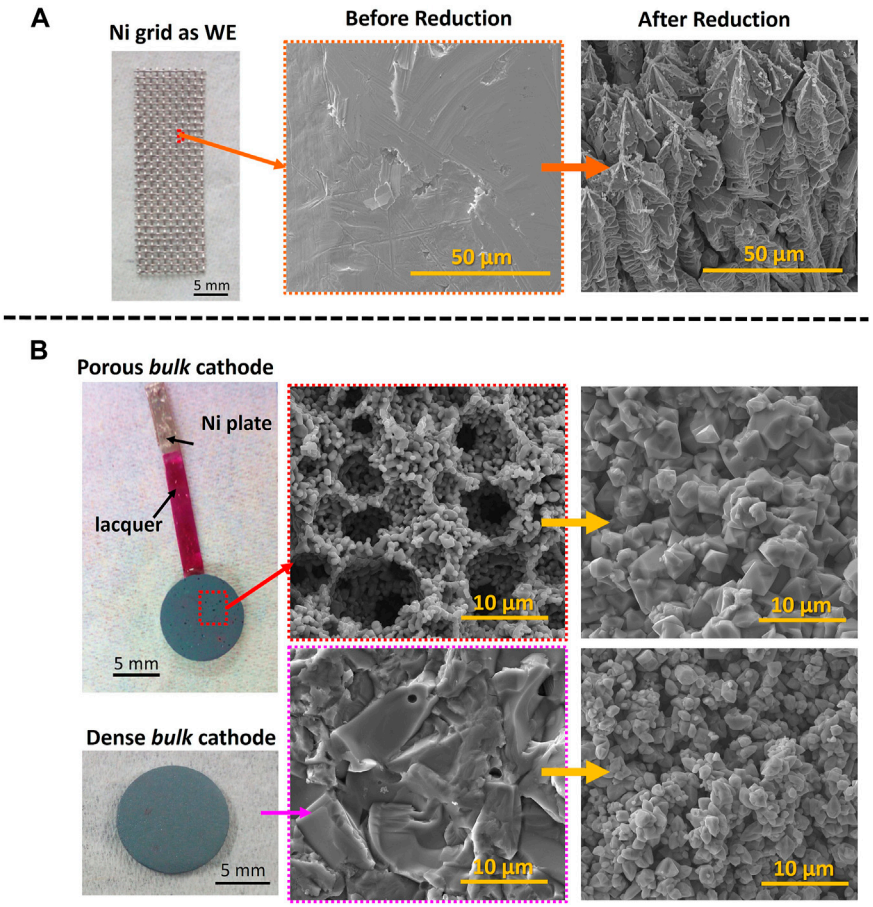

FIGURE 1
Microstructural evolution of the Working Electrode (WE) during the electrochemical reduction to Fe in 10 M NaOH and at 90°C in a **(A)** Fe_2O_3 ceramic suspension and as a **(B)** Fe_2O_3 ceramic bulk cathode.

Electroreduction from iron oxide-based suspensions

The overall electroreduction mechanism involves two stages: reduction of Fe(III) to Fe(II) species followed by further reduction and cathodic deposition of iron (Gorbunova and Liamina, 1966; Armstrong and Baurhoo, 1972). Thermodynamic studies (Diakonov et al., 1999) proposed the hydrolysis of Fe_2O_3 in alkaline solutions to $Fe(OH)_4^-$. However, the low solubility of Fe_2O_3 in alkaline conditions (~2×10^{-3} M at 18 M NaOH, 100°C (Picard et al., 1980b)) raised concerns regarding this mechanism. Since then, significant advances in understanding this process have been made. Today the main emphasis is given to a dissolution/redeposition route and solid-state mechanism. Thus, the preliminary dissolution of Fe_2O_3 and formation of $Fe(OH)_4^-$ is considered (Picard et al., 1980a; Le and Ghali, 1993; Beverskog and Puigdomenech, 1996; Diakonov et al., 1999; Allanore et al., 2007; Yuan et al., 2009; Yuan and Haarberg, 2009), as $Fe_2O_3 + 3H_2O + 2OH^- \rightleftharpoons 2Fe(OH)_4^-$. The second step consists of the reduction of the $Fe(OH)_4^-$ to $Fe(OH)_3^-$ in solution, $Fe(OH)_4^- + e^- \rightarrow Fe(OH)_3^- + OH^-$, followed by complete reduction and cathodic deposition of Fe, $Fe(OH)_3^- + 2e^- \rightarrow Fe^0 + 3OH^-$ (Le and Ghali, 1993; Beverskog and Puigdomenech, 1996; Allanore et al., 2007).

A second proposed reduction mechanism involves the adsorption of Fe_2O_3 particles at the WE's surface. Around 3 min of the WE immersion in a Fe_2O_3 suspension was enough to form Fe deposits after a potentiostatic electroreduction (−1.2 V vs. Hg|HgO) in a separate particle-free cell (Allanore et al., 2010a). The adsorption effect is caused by electrostatic forces, since the Fe_2O_3 particles have a slightly positive zeta potential in strong alkaline media, in contrast with the negatively charged WE (Siebentritt et al., 2014). This second route is expected to occur simultaneously with the first route, despite not being mentioned very often. Alkali concentration, cell operating temperature, and iron oxide load are the main factors determining the contribution of each mechanism to the overall process. Working electrodes (WE) as

graphite (Allanore et al., 2007; Yuan et al., 2009; Tokushige et al., 2013; Feynerol et al., 2017; Maihatchi et al., 2020), Cu rod (Zou et al., 2015a), *Fe rod* (Ivanova et al., 2015), stainless steel plates (Koutsoupa et al., 2021a; 2021b) or Ni grids (Lopes et al., 2020, 2021, 2022) are usually used. Dendritic/star-like shape Fe deposits are often obtained after the electrochemical reduction of iron oxides in alkaline suspensions (Figure 1A).

Bulk electroreduction

The bulk electroreduction refers to *in situ* conversion of iron ore pieces or lumps, acting as a cathode (or WE), to Fe. The microstructure of such cathodes is often decisive for electroreduction. The low electrical conductivity of Fe_2O_3 (10^{-14} S/cm (Morin, 1951; Lee et al., 2012)) requires a mechanical connection between the iron oxide piece and the electrochemical cell. A three-phase interlines (3PIs) model is often used for explaining the electrochemical reduction of typical solid insulators (Deng et al., 2005; Xiao et al., 2007; Zou et al., 2015b). Thus, the insulating Fe_2O_3 can only be reduced after establishing an interface with an electrical conductor (*e.g.* metal attached to the pellet acting as a current collector) and simultaneously with an electrolyte. Electrically conductive metals such as Ni (Ivanova et al., 2017; Lopes et al., 2018) or steel (Allanore et al., 2008) are frequently used as current collectors.

Chronoamperometry studies of iron electroreduction allow understanding of the bulk shrinking behaviour of iron oxide-based cathodes during Fe formation, where three well-defined regions are visible in the current density vs. time plot (Allanore et al., 2010c; Zou et al., 2015b). Corresponding steps include: i) electrolyte entrance to the external layer of the cathode and expansion of the 3PIs model along the surface; ii) cathode surface reduction to form metallic Fe; iii) the unreduced core is finally reduced to Fe leading to a shrinking of the cathode. The current density is then stabilized, resulting in the "shrinking-core reaction process" proposed by Zou and his co-workers.

Magnetite Fe_3O_4 phase (10^3 S/cm (Cornell and Schwertmann, 2003; Lee et al., 2012)) is often observed as an intermediate phase during Fe_2O_3 electroreduction. It is responsible for boosting the current density in the second step of the shrinking-core process. Most authors consider the dissolution-electrodeposition route even in the case of bulk electroreduction (Sato et al., 1970; Schmuki et al., 1996; Allanore et al., 2010c; Zou et al., 2015b, 2015a; Ivanova et al., 2017), where Fe_3O_4 phase undergoes a reductive dissolution to Fe(II) aqueous species as $Fe(OH)_3^-$ (Allen et al., 1980). The Fe(II) species react with the neighbouring bulk Fe_2O_3 promoting new Fe_3O_4 phase formation. However, other authors (He et al., 2011; Haarberg and Yuan, 2014) consider a solid-state Fe_3O_4 reduction to Fe. Zou and his co-workers do not completely exclude this route but strongly highlight the main reduction pathway as the dissolution-electrodeposition (Zou et al., 2015b; 2015a). Other Fe(II) species forming during Fe_3O_4 reduction ($HFeO_2^-$, etc) are also considered and predicted by Pourbaix diagrams (Pourbaix, 1974; Le and Ghali, 1993). On the other hand, $Fe(OH)_2$ is mostly present at working temperatures below 65°C (Schrebler Guzmán et al., 1979; Le and Ghali, 1993; Zhang and Park, 1994).

Another relevant aspect of the electrochemical reduction of bulk cathodes refers to the porosity increase of around 30–50% when Fe is formed (Allanore et al., 2008; 2010c), promoted by significant density change from Fe_2O_3 phase (5.26 g/cm^3) to Fe (7.86 g/cm^3). The space between the Fe particles becomes wider with the growth of these Fe microstructures in a dendrite shape, increasing the porosity of the metal (Zou et al., 2015a). The electrolyte presence was found between the metal iron oxide layer interface (Allanore et al., 2010c), which can also be crucial when considering the initial porosity of the bulk cathodes. Thus, the processing conditions should ideally provide some connectivity between even residual pores to ensure the percolation of the electrolyte and ionic species inside the cathode towards the current collector (Zou et al., 2015b). When cellular iron oxide-based designed cathodes with open porosities higher than 37 vol% are used (Ivanova et al., 2017; Lopes et al., 2019, 2021, 2022), the electroreduction is facilitated, and the forming Fe crystals preserve the original cellular-based ceramics microstructure, suggesting that the reductive dissolution to Fe(II) occurs in sub-micrometer distances. The porosity of 37 vol% was found to ensure the best performance towards electroreduction, while maintaining suitable mechanical properties of the ceramic cathodes, leading to complete conversion of the ceramic cathode to metallic Fe (Lopes et al., 2019). The Fe microstructure evolution when considering dense or porous bulk ceramic cathodes is demonstrated in Figure 1B.

Factors affecting the faradaic efficiency of the electroreduction

Hydrogen evolution reaction (HER; $2H_2O + 2e^- \rightarrow H_2 + 2OH^-$) has a parasitic effect on iron electroreduction due to the superimposed cathodic potential region with the reduction to Fe. In fact, the first couple of hours of a cathodic polarization are ascribed to hydrogen adsorption at the cathode, leading to a higher overvoltage (Brossard and Huot, 1991; Allanore et al., 2007). HER is the main factor responsible for the loss of Faradaic efficiency, lowering the quality of Fe deposits. Although it is not possible to eliminate, minimizing HER until a certain level is feasible. The choice of the cathode is of great relevance when considering the electrodeposition from suspensions. Noble metals (Pt, Pd, or Nu) have low HER activity, while Fe, Ni, Co, Au, and Ag have moderate activity. On the other hand, Zn, Ti, Zn, Pb, or Sn have high overpotentials (Ivanova et al., 2015; Rashid et al., 2015). The use of rotation disk electrodes (RDE) (up to

TABLE 1 Comparison of the Faradaic Efficiencies between traditional and alternative iron oxide feedstocks.

	Iron feedstock	Type of electroreduction	WE	Experimental conditions	Faradaic efficiency	Ref
Traditional feedstock	Fe_2O_3	Suspension	Graphite rotating disk	18 M NaOH; T = 114°C; 1,000 rpm; j = 4000 A/m^2; 33 wt% Fe_2O_3	95%	Yuan et al. (2009)
	Fe_2O_3 iron ore lumps	Bulk	Ore lump + Ni	18 M NaOH; T = 100°C; E = −1.20 V (vs SHE)	53–100%	Allanore et al. (2010c)
	Fe_2O_3	Suspension	Graphite rotating disk	18 M NaOH; T = 110°C; 1,000 rpm; j = 1,000–6000 A/m^2; 33 and 40 wt% Fe_2O_3	95% (40 wt% Fe_2O_3 + 3000 A/m^2)	Tokushige et al. (2013)
	Fe_3O_4	Bulk	Fe_3O_4 pellets sintered at 1,100–1,400°C + Ni foil	10 M NaOH; T = 90°C; E = -1.15 V (vs Hg|HgO)	85% (pellets with 22% of open porosity)	Monteiro et al. (2016)
	Fe_2O_3 Fe_3O_4 α-FeOOH	Suspension	Graphite rod	18 M NaOH; T = 110°C; 600 rpm; E = −1.66 V; 10 wt% of iron oxides	86% (Fe_2O_3) 5% (Fe_3O_4) 66% (α-FeOOH)	Feynerol et al. (2017)
	Fe_2O_3	Bulk	Fe_2O_3 porous pellets fired at 1,100–1,200°C + Ni foil	10 M NaOH; T = 90°C; E = −1.15 V and -1.50 V (vs Hg|HgO)	39% (E = -1.15 V) 21% (E = -1.50 V)	Ivanova et al. (2017)
Alternative feedstock	Red Mud	Suspension	Graphite rod with Ti/Pt grid	12.5 M NaOH; T = 110°C; 600 rpm; j = 45 A/m^2; 333.3 g/L of red mud	71% for red mud (45 A/m^2) ~80% for Fe_2O_3 (200–1000 A/m^2)	Maihatchi et al. (2020)
	Titanomagnetite from iron sands	Bulk	Iron sand + stainless steel	18 M NaOH; T = 110°C; j = 1 A/cm^2	Very low	Bjareborn et al. (2020)
	Red Mud	Suspension	Stainless steel plate	18 M NaOH; T = 70–130°C; 500 rpm; j = 138 and 1100 A/m^2; 10 wt% of red mud or Fe_2O_3	~80% for Fe_2O_3 regardless the temperature (138 A/m^2); ~10% (70°C) to 70% (130°C) for red mud (138 A/m^2)	Koutsoupa et al. (2021a)
	Pseudobrookite	Bulk	Fe_2TiO_5 + Ni plate	10 M NaOH; T = 80°C; E = −1.30 V (vs Hg|HgO)	Very low	Lopes et al. (2022)
	Pseudobrookite	Suspension	Steel rod	10 M NaOH; T = 80°C; 100 rpm; E = -1.15 V (vs Hg|HgO); 100 g/L of iron oxide	25%	
	Iron oxide residues from Zn production	Suspension	Graphite rotating disk and silver rod	18 M NaOH; T = 110°C; 500 rpm for rotating disk +100 rpm for magnetic stirrer; E = -1.6 V	-	Haarberg et al. (2022)
	Iron oxide residues from Ni production	Suspension	Graphite rotating disk and silver rod	18 M NaOH; T = 110°C; 500 rpm for rotating disk +100 rpm for magnetic stirring; j = 0.6 A/cm^2; 1: 90 g/L of residue	7%	

3,000 rpm) lowers the Faradaic efficiencies from 96% (<1,000 rpm) to 76% (3,000 rpm) due to the combined effect of air and H_2 bubbles at its surfaces (Yuan et al., 2009). RDE also restrict the transport of the suspended particles around the WE (Allanore et al., 2010b). Stirring conditions below 2000 rpm allow to maintain high current efficiency, according to Yuan et al. Moreover, the bubbles can also have a negative impact on the electroreduction by dropping the current density due to the vibration of the ceramic cathodes (Allanore et al., 2010c). However, increasing the porosity of the cathode for the bulk electroreduction allowed the bubbles to escape through the pores, representing one alternative way to minimize this effect (Ivanova et al., 2017).

HER potentials tend to increase for higher cathodic values when the alkaline electrolyte concentrations increase (Nickell et al., 2006). Some authors have been employing 18 M NaOH electrolyte solutions (Allanore et al., 2008, 2010c; Yuan et al., 2009; Tokushige et al., 2013) to minimize the HER effect. Although increasing the concentration of the electrolyte seems to decrease the HER impact and, consequently, the Faradaic efficiency increase, it does not guarantee itself a high efficiency level as, for example, ~70% of efficiency was obtained at 18 M NaOH (Allanore et al., 2007) and ~80% at 10 M NaOH (Ivanova et al., 2015). On the other hand, current efficiency drop from 39% to 21% when potentiostatic cathodic polarizations of -1.15 V and -1.50 V (vs Hg|HgO) are used, respectively, in 10 M NaOH

solutions (Ivanova et al., 2017). This aspect clearly demonstrates the increased HER contribution at higher polarizations for the same electrolyte concentration. The efficiency also increases for higher iron oxide concentration in the alkaline suspension (Allanore et al., 2007). In general, the Faradaic efficiency is a complex parameter affected by the cell configuration, type of electrodes, iron oxide load, current densities or cathodic polarizations applied, and temperature.

Alternative iron feedstocks and their suitability

An overview analysis of potential feedstocks for electrolytic iron production is given in Table 1. Hematite is a reference iron oxide feedstock for the electrochemical reduction studies in alkaline media showing high efficiencies (>85%), except at high cathodic polarizations (*e.g.* 39% at −1.15 V) due/to HER contribution. Iron (hydroxy-) oxides such as Fe_3O_4 and α-FeOOH (goethite) also can be used as raw material in suspensions (Feynerol et al., 2017), with consequently lower current efficiencies due to the magnetic behaviour of the particles and high viscosity that restricts the evolution of O_2 bubbles, respectively. Latest studies on alternative feedstocks include the use of industrial iron-rich waste as red mud from the Bayer process (Maihatchi et al., 2020; Koutsoupa et al., 2021a, 2021b) and iron-rich residues from the Zn and Ni electrowinning industrial production (Haarberg et al., 2022). The use of iron-rich waste is of high interest due to the possibility of waste valorisation, which is strongly supported by the European Commission and contributes to the circular economy. Faradaic efficiencies of red mud reach about 70%, but only when low current density is applied (45–138 A/m^2) in concentrated electrolytes (>12.5 M). On the other hand, titanomagnetite from natural ironsands (Bjareborn et al., 2020) showed low efficiencies. In fact, significant challenges are imposed when considering various alternative feedstocks. The presence of non-conductive phases suppresses the electroreduction to metallic iron. Ni and Zn residues from industrial production show low efficiencies (<7%) even when considering pre-treatments of both wastes. Several iron-oxide based compositions have been the research aim under the SIDERWIN European project for electrolytic iron production in alkaline media. The impact of Al- (Lopes et al., 2019, 2020), Mg- (Lopes et al., 2021), and Ti- (Lopes et al., 2022) additions to iron-oxide ceramic cathodes and/or suspensions have been investigated. The dissolution of the mentioned species to the electrolyte leads to the partial blocking of the cathode surface, restricting further reduction to Fe. The Ti- blocking effect strongly affects the conversion of the synthetic pseudobrookite mineral (Fe_2TiO_5), where simply Fe_3O_4 phase (intermediary phase) was found at -1.15 V (Lopes et al., 2022). Strong cathodic polarizations were required for producing Fe from Fe_2TiO_5 suspensions with consequent impact on the faradaic efficiencies (<25%) due to HER.

Concluding remarks

Fast implementation of clean energy technologies in steelmaking requires developing cost-effective approaches. Although the recent research results and trends show that metallic iron production by electrolysis is a feasible approach, many experimental challenges still need to be resolved. Up to now, high and reproducible Faradaic efficiencies have been achieved mostly when using pure iron oxides as a feedstock. The presence of impurities harms the current yield, and the detailed relevant mechanisms and corresponding mitigation strategies are still to be discovered. At the same time, the possibility of achieving high Faradaic efficiency while using red mud as an iron feedstock was recently demonstrated, confirming the potential sustainability of the proposed technology and its contribution to the circular economy. It must be noticed that, in commonly used alkaline conditions, the efficiency of iron electroreduction is compromised only by the cathodic evolution of hydrogen gas, which may be considered the fuel of the future, with no carbon footprint, highest enthalpy of combustion, and releasing water as a by-product during energy release. Thus, even if the current efficiency of iron production is still relatively low, the electrolysis process can be potentially adapted to the intermittency of renewable energies and optimized towards iron electroreduction or green hydrogen production, depending on the actual power conditions. This opens new prospects for this approach as a green alternative to traditional steelmaking, where breakthrough technologies are urgent and necessary. The electrolytic iron production arises as a competitive technology against the conventional technology by saving 6 GJ/ton of Fe produced, representing a turning point in the metallurgical industry in the near future. de Beer, 2000.

Author contributions

DVL and AVK contributed to the design and conceptualization of the minireview. DVL and AVK wrote the draft of the manuscript. MJQ and JRF improved specific sections of the minireview. All authors contributed to the minireview revision and approved the submitted version.

Funding

This work was developed within the scope of the European SIDERWIN project (SIDERWIN- DLV-768788 - Horizon 2020/SPIRE10), and CICECO-Aveiro Institute of Materials, UIDB/

50011/2020 and UIDP/50011/2020, and LA/P/0006/2020, financed by national funds through the FCT/MEC (PIDDAC).

Conflict of interest

The authors declare that the research was conducted in the absence of any commercial or financial relationships that could be construed as a potential conflict of interest.

Publisher's note

References

Allanore, A., Feng, J., Lavelaine, H., and Ogle, K. (2010a). The adsorption of hematite particles on steel in strongly alkaline electrolyte. *J. Electrochem. Soc.* 157, E24–E30. doi:10.1149/1.3273198

Allanore, A., Lavelaine, H., Birat, J. P., Valentin, G., and Lapicque, F. (2010b). Experimental investigation of cell design for the electrolysis of iron oxide suspensions in alkaline electrolyte. *J. Appl. Electrochem.* 40, 1957–1966. doi:10.1007/s10800-010-0172-0

Allanore, A., Lavelaine, H., Valentin, G., Birat, J. P., Delcroix, P., and Lapicque, F. (2010c). Observation and modeling of the reduction of hematite particles to metal in alkaline solution by electrolysis. *Electrochim. Acta* 55, 4007–4013. doi:10.1016/j.electacta.2010.02.040

Allanore, A., Lavelaine, H., Valentin, G., Birat, J. P., and Lapicque, F. (2007). Electrodeposition of metal iron from dissolved species in alkaline media. *J. Electrochem. Soc.* 154, E187–E193. doi:10.1149/1.2790285

Allanore, A., Lavelaine, H., Valentin, G., Birat, J. P., and Lapicque, F. (2008). Iron metal production by bulk electrolysis of iron ore particles in aqueous media. *J. Electrochem. Soc.* 155, E125–E129. doi:10.1149/1.2952547

Allen, P. D., Bignold, G. J., and Hampson, N. A. (1980). The electrodissolution of magnetite: Part III. Iron nucleation processes on magnetite electrodes. *J. Electroanal. Chem. Interfacial Electrochem.* 112, 239–246. doi:10.1016/S0022-0728(80)80405-0

Angel, E. (1952). *US Patent No 2,622,063, Electrolytic production of iron and iron alloys*. Washington, D.C: United States Patent Office.

Armstrong, R., and Baurhoo, I. (1972). The dissolution of iron in concentrated alkali. *J. Electroanal. Chem. Interfacial Electrochem.* 40, 325–338. doi:10.1016/S0022-0728(72)80377-2

Beer, J. (2000). *Eco-efficency in industry and science*. Dordrecht, Utrecht, Netherlands: Springer. doi:10.1007/978-94-017-2728-0

Beverskog, B., and Puigdomenech, I. (1996). Revised Pourbaix diagrams for ion at 25-300 °C. *Corros. Sci.* 38, 2121–2135. doi:10.1016/S0010-938X(96)00067-4

Bjareborn, O., Arif, T., Monaghan, B., and Bumby, C. W. (2020). Fate of titanium in alkaline electro-reduction of sintered titanomagnetite. *Mat. Res. Express* 7, 106508. doi:10.1088/2053-1591/abbd24

Brossard, L., and Huot, J. Y. (1991). *In situ* activation of cathodes during alkaline water electrolysis by dissolved iron and molybdenum species. *J. Appl. Electrochem.* 21, 508–515. doi:10.1007/BF01018603

Cavaliere, P. (2019). *Clean ironmaking and steelmaking processes*. Italy: LecceSpringer International Publishing. doi:10.1007/978-3-030-21209-4

Cornell, R. M., and Schwertmann, U. (2003). *The iron oxides: Structres, properties, reactions, occurences and uses*. Second Edi. Weinheim: Wiley VCH. doi:10.1002/3527602097

de Beer, J. (2000). Potential for industrial energy-efficiency improvement in the long term. *Eco Effi. Ind. and Sci.* 5. doi:10.1007/978-94-017-2728-0

Deng, Y., Wang, D., Xiao, W., Jin, X., Hu, X., and Chen, G. Z. (2005). Electrochemistry at conductor/insulator/electrolyte three-phase interlines: A thin layer model. *J. Phys. Chem. B* 109, 14043–14051. doi:10.1021/jp044604r

Diakonov, I. I., Schott, J., Martin, F., Harrichourry, J. C., and Escalier, J. (1999). Iron(III) solubility and speciation in aqueous solutions. Experimental study and modelling: Part 1. Hematite solubility from 60 to 300??C in NaOH-NaCl solutions and thermodynamic properties of Fe(OH)4-(aq). *Geochim. Cosmochim. Acta* 63, 2247–2261. doi:10.1016/S0016-7037(99)00070-8

Díaz, S. L., Calderón, J. A., Barcia, O. E., and Mattos, O. R. (2008). Electrodeposition of iron in sulphate solutions. *Electrochim. Acta* 53, 7426–7435. doi:10.1016/j.electacta.2008.01.015

Draxler, M., Schenk, J., Bürgler, T., and Sormann, A. (2020). The steel industry in the European union on the crossroad to carbon lean production—status, initiatives and challenges. *Berg. Huettenmaenn. Monatsh.* 165, 221–226. doi:10.1007/s00501-020-00975-2

Elavarasan, R. M., Pugazhendhi, R., Irfan, M., Mihet-Popa, L., Khan, I. A., and Campana, P. E. (2022). State-of-the-art sustainable approaches for deeper decarbonization in Europe – an endowment to climate neutral vision. *Renew. Sustain. Energy Rev.* 159, 112204. doi:10.1016/j.rser.2022.112204

Estelle, A. (1915). *Swedish Patent No 42,849, Förfarande för framställning av järn genom elektrolytisk reduktion i lösning av kaustikt alkali*. Stockholm: Kungl. Patent och Registreringsverket.

Fan, Z., and Friedmann, S. J. (2021). Low-carbon production of iron and steel: Technology options, economic assessment, and policy. *Joule* 5, 829–862. doi:10.1016/j.joule.2021.02.018

Feynerol, V., Lavelaine, H., Marlier, P., Pons, M. N., and Lapicque, F. (2017). Reactivity of suspended iron oxide particles in low temperature alkaline electrolysis. *J. Appl. Electrochem.* 47, 1339–1350. doi:10.1007/s10800-017-1127-5

Gamburg, Y., and Zangari, G. (2011). *Theory and practice of metal electrodeposition*. London: Springer Science+Business Media, LLC. doi:10.1017/CBO9781107415324.004

Gorbunova, K. M., and Liamina, L. I. (1966). On the mechanism of iron reduction from alkaline solutions. *Electrochim. Acta* 11, 457–467. doi:10.1016/0013-4686(66)80023-3

Haarberg, G. M., Qin, B., and Khalaghi, B. (2022). "Electrochemical reduction of iron oxides in aqueous NaOH electrolyte including iron residue from nickel and zinc electrowinning processes," in *Rare metal technology 2022. The minerals, metals & materials series* (Cham: Springer), 341–347. doi:10.1007/978-3-030-92662-5_33

Haarberg, G. M., and Yuan, B. (2014). Direct electrochemical reduction of hematite pellets in alkaline solutions. *ECS Trans.* 58, 19–28. doi:10.1149/05820.0019ecst

He, Z., Gudavarthy, R. V., Koza, J. A., and Switzer, J. A. (2011). Room-temperature electrochemical reduction of epitaxial magnetite films to epitaxial iron films. *J. Am. Chem. Soc.* 133, 12358–12361. doi:10.1021/ja203975z

HORIZON2020 (2020). EU coordinated methods and procedures based on real cases for the effective implementation of policies and measures supporting energy efficiency in the Industry. *Technical analysis – iron and steel sector*. NACE C24.1-24.2-24-5, 18.

Ivanova, Y., Monteiro, J., Horovistiz, A., Ivanou, D., Mata, D., Silva, R., et al. (2015). Electrochemical deposition of Fe and Fe/CNTs composites from strongly alkaline hematite suspensions. *J. Appl. Electrochem.* 45, 515–522. doi:10.1007/s10800-015-0803-6

Ivanova, Y., Monteiro, J., Teixeira, L., Vitorino, N., Kovalevsky, A., and Frade, J. (2017). Designed porous microstructures for electrochemical reduction of bulk hematite ceramics. *Mat. Des.* 122, 307–314. doi:10.1016/j.matdes.2017.03.031

Izaki, M. (2010). "Electrodeposition of iron and iron alloys," in *Modern electroplating*. Editors M. Schlesinger and M. Paunovic (John Wiley & Sons), 309–326. doi:10.1007/BF01022244

Koutsoupa, S., Koutalidi, S., Balomenos, E., and Panias, D. (2021a). Σiderwin — a new route for iron production. *Mat. Proc.* 5, 58. doi:10.3390/materproc2021005058

Koutsoupa, S., Koutalidi, S., Bourbos, E., Balomenos, E., and Panias, D. (2021b). Electrolytic iron production from alkaline bauxite residue slurries at low temperatures : Carbon-free electrochemical process for the production of

metallic iron. *Johns. Matthey Technol. Rev.* 65, 366–374. doi:10.1595/205651320X15918757312944

Lavelaine, H., Van der Laan, S., Hita, A., Olsen, K., Serna, M., Haarberg, G., et al. (2016). *Iron production by electrochemical reduction of its oxide for high CO2 mitigation (IERO)*. Brussels: European Comission.

Le, H., and Ghali, E. (1993). Interpretation des diagrammes E-pH du systeme Fe-H2O en relation avec la fragilisation caustique des aciers. *J. Appl. Electrochem.* 23, 72–77. doi:10.1007/BF00241579

Lee, K. K., Deng, S., Fan, H. M., Mhaisalkar, S., Tan, H. R., Tok, E. S., et al. (2012). α-Fe2O3 nanotubes-reduced graphene oxide composites as synergistic electrochemical capacitor materials. *Nanoscale* 4, 2958–2961. doi:10.1039/c2nr11902a

Lopes, D. V., Ivanova, Y. A., Kovalevsky, A. V., Sarabando, A. R., Frade, J. R., and Quina, M. J. (2019). Electrochemical reduction of hematite-based ceramics in alkaline medium: Challenges in electrode design. *Electrochim. Acta* 327, 135060. doi:10.1016/j.electacta.2019.135060

Lopes, D. V., Kovalevsky, A., Quina, M., and Frade, J. (2020). Electrochemical deposition of zero-valent iron from alkaline ceramic suspensions of Fe2-xAlxO3 for iron valorisation. *J. Electrochem. Soc.* 167, 102508. doi:10.1149/1945-7111/ab9a2b

Lopes, D. V., Kovalevsky, A. V., Quina, M. J., and Frade, J. R. (2018). Processing of highly-porous cellular iron oxide-based ceramics by emulsification of ceramic suspensions. *Ceram. Int.* 44, 20354–20360. doi:10.1016/j.ceramint.2018.08.024

Lopes, D. V., Lisenkov, A. D., Ruivo, L. C. M., Yaremchenko, A. A., Frade, J. R., and Kovalevsky, A. V. (2022). Prospects of using pseudobrookite as an iron-bearing mineral for the alkaline electrolytic production of iron. *Mater. (Basel)* 15, 1440. doi:10.3390/ma15041440

Lopes, D. V., Lisenkov, A. D., Sergiienko, S. A., Constantinescu, G., Sarabando, A., Quina, M. J., et al. (2021). Alkaline electrochemical reduction of a magnesium ferrospinel into metallic iron for the valorisation of magnetite-based metallurgical waste. *J. Electrochem. Soc.* 168, 073504. doi:10.1149/1945-7111/ac1490

Maihatchi, A., Pons, M.-N., Ricoux, Q., Goettmann, F., and Lapicque, F. (2020). Electrolytic iron production from alkaline suspensions of solid oxides: Compared cases of hematite, iron ore and iron-rich bayer process residues. *J. Electrochem. Sci. Eng.* 10, 95–102. doi:10.5599/jese.751

Mandin, P., Wüthrich, R., and Roustan, H. (2019). Industrial aluminium production: The Hall-heroult process modelling. *ECS Trans.* 19, 1–10. doi:10.1149/1.3247986

Monhemius, A. J. (1980). "The electrolytic production of chlorates," in *Topics in non-ferrous extractive metallurgy*. Editor A. R. Burkin (Oxford, UK: Blackwell Scientific Publications), 104–130. doi:10.1038/scientificamerican08021902-22233asupp

Monteiro, J., Ivanova, Y., Kovalevsky, A., Ivanou, D., and Frade, J. (2016). Reduction of magnetite to metallic iron in strong alkaline medium. *Electrochim. Acta* 193, 284–292. doi:10.1016/j.electacta.2016.02.058

Morin, F. (1951). Electrical properties ofαFe2O3andαFe2O3Containing titanium. *Phys. Rev.* 83, 1005–1010. doi:10.1103/PhysRev.83.1005

Mousa, E. A. (2019). Modern blast furnace ironmaking technology: Potentials to meet the demand of high hot metal production and lower energy consumption. *Metall. Mat. Eng.* 25, 69–104. doi:10.30544/414

Müller, C. I., Sellschopp, K., Tegel, M., Rauscher, T., Kieback, B., and Röntzsch, L. (2016). The activity of nanocrystalline Fe-based alloys as electrode materials for the hydrogen evolution reaction. *J. Power Sources* 304, 196–206. doi:10.1016/j.jpowsour.2015.11.008

Nickell, R. A., Zhu, W. H., Payne, R. U., Cahela, D. R., and Tatarchuk, B. J. (2006). Hg/HgO electrode and hydrogen evolution potentials in aqueous sodium hydroxide. *J. Power Sources* 161, 1217–1224. doi:10.1016/j.jpowsour.2006.05.028

Picard, G., Oster, D., and Tremillon, B. (1980a). Electrochemical reduction of iron oxides in suspension in water-sodium hydroxide mixtures between 25 and 140 °C. I: Theoretical study. *J. Chem. Res.* 8, 250–251.

Picard, G., Oster, D., and Tremillon, B. (1980b). Electrochemical reduction of iron oxides in suspension in water-sodium hydroxide mixtures between 25 and 140 °C. II: Experimental study. *J. Chem. Res.* 8, 252–253.

Pourbaix, M. (1974). *Atlas of electrochemical equilibria in aqueous solutions*. 2nd Editio. Brussels: Cebelcor Brussels.

Quader, M. A., Ahmed, S., Dawal, S. Z., and Nukman, Y. (2016). Present needs, recent progress and future trends of energy-efficient Ultra-Low Carbon Dioxide (CO2) Steelmaking (ULCOS) program. *Renew. Sustain. Energy Rev.* 55, 537–549. doi:10.1016/j.rser.2015.10.101

Rashid, M. M., Al Mesfer, M. K., Naseem, H., and Danish, M. (2015). Hydrogen production by water electrolysis: A review of alkaline water electrolysis, pem water electrolysis and high temperature water electrolysis. *Int. J. Eng. Adv. Technol.*, 2249–8958.

Sato, N., Kudo, K., and Noda, T. (1970). Single layer of the passive film on Fe. *Corros. Sci.* 10, 785–794. doi:10.1016/S0010-938X(70)80002-6

Schmuki, P., Virtanen, S., Davenport, A., and Vitus, C. (1996). *In situ* X-ray absorption near-edge spectroscopic study of the cathodic reduction of artificial iron oxide passive films. *J. Electrochem. Soc.* 143, 574–582. doi:10.1149/1.1836483

Schrebler Guzmán, R. S., Vilche, J. R., and Arvía, A. J. (1979). The potentiodynamic behaviour of iron in alkaline solutions. *Electrochim. Acta* 24, 395–403. doi:10.1016/0013-4686(79)87026-7

Shafer, W., and Harr, C. (1958). Electrolytic iron powders-production and properties. *J. Electrochem. Soc.* 105, 413–417. doi:10.1149/1.2428876

SIDERWIN (2022). SIDERWIN. Available at: https://www.siderwin-spire.eu/.

Siebentritt, M., Volovitch, P., Ogle, K., and Lefèvre, G. (2014). Adsorption and electroreduction of hematite particles on steel in strong alkaline media. *Colloids Surfaces A Physicochem. Eng. Aspects* 440, 197–201. doi:10.1016/j.colsurfa.2012.09.002

Su, C.-w., He, F.-j., Ju, H., Zhang, Y.-b., and Wang, E.-l. (2009). Electrodeposition of Ni, Fe and Ni-Fe alloys on a 316 stainless steel surface in a fluorborate bath. *Electrochim. Acta* 54, 6257–6263. doi:10.1016/j.electacta.2009.05.076

Tokushige, M., Kongstein, O. E., and Haarberg, G. M. (2013). Crystal orientation of iron produced by electrodeoxidation of hematite particles. *ECS Trans.* 50, 103–114. doi:10.1149/05052.0103ecst

U.S. Department of Energy (2014). *Advanced manufacturing office (AMO)*. Washington, D.C: U.S. Department of Energy.

World Steel Association (2022). *World steel in figures*. Brussels: Worldsteel Association.

Xiao, W., Jin, X., Deng, Y., Wang, D., and Chen, G. Z. (2007). Three-phase interlines electrochemically driven into insulator compounds: A penetration model and its verification by electroreduction of solid AgCl. *Chem. Eur. J.* 13, 604–612. doi:10.1002/chem.200600172

Yuan, B., and Haarberg, G. (2009). Electrodeposition of iron in aqueous alkaline solution: An alternative to carbothermic reduction. *ECS Trans.* 16, 31–37. doi:10.1149/1.3114006

Yuan, B., Kongstein, O. E., and Haarberg, G. M. (2009). Electrowinning of iron in aqueous alkaline solution using a rotating cathode. *J. Electrochem. Soc.* 156, D64–D69. doi:10.1149/1.3039998

Zhang, H., and Park, S. M. (1994). Rotating ring-disk electrode and spectroelectrochemical studies on the oxidation of iron in alkaline solutions. *J. Electrochem. Soc.* 141, 718–724. doi:10.1149/1.2054798

Zou, X., Gu, S., Cheng, H., Lu, X., Zhou, Z., Li, C., et al. (2015a). Facile electrodeposition of iron films from NaFeO2 and Fe2O3 in alkaline solutions. *J. Electrochem. Soc.* 162, D49–D55. doi:10.1149/2.0751501jes

Zou, X., Gu, S., Lu, X., Xie, X., Lu, C., Zhou, Z., et al. (2015b). Electroreduction of iron (III) oxide pellets to iron in alkaline media : A typical shrinking-core reaction process. *Metall. Materi. Trans. B* 46B, 1262–1274. doi:10.1007/s11663-015-0336-8